

Towards Scalable Insect Monitoring: Ultra-Lightweight CNNs as On-Device Triggers for Insect Camera Traps

Ross Gardiner¹, Sareh Rowlands², Benno I. Simmons³

¹ Environmental Intelligence CDT, University of Exeter, UK

² Institute for Data Science and AI, University of Exeter, UK

³ Centre for Ecology and Conservation, University of Exeter, UK

Abstract

1. Camera traps, combined with AI, have emerged as a way to achieve automated, scalable biodiversity monitoring. However, the passive infrared (PIR) sensors that trigger camera traps are poorly suited for detecting small, fast-moving ectotherms such as insects. Insects comprise over half of all animal species and are key components of ecosystems and agriculture. The need for an appropriate and scalable, insect camera trap is critical in the wake of concerning reports of declines in insect populations.
2. This study proposes an alternative to the PIR trigger: ultra-lightweight convolutional neural networks running on low-powered hardware to detect insects in a continuous stream of captured images. We train a suite of models to distinguish insect images from backgrounds. Our design achieves zero latency between trigger and image capture.
3. Our models are rigorously tested and achieve high accuracy ranging from 91.8% to 96.4% AUC on validation data and >87% AUC on data from distributions unseen during training. The high specificity of our models ensures minimal saving of false positive images, maximising deployment storage efficiency. High recall scores indicate a minimal

false negative rate, maximising insect detection. Further analysis using saliency maps shows the learned representation of our models to be robust, with low reliance on spurious background features. Our system is also shown to operate deployed on off-the-shelf, low-powered microcontroller units, consuming a maximum power draw of less than 300mW. This enables longer deployment times using cheap and readily available battery components.

4. Overall we offer a step change in the cost, efficiency and scope of insect monitoring. By solving the challenging trigger problem, we demonstrate a system which can be deployed for far longer than existing designs and budgets power and bandwidth effectively, moving towards a generic camera trap for insects.

along with the code-base and all realised models will be uploaded to the Data Dryad platform upon acceptance at:

Keywords

Artificial Intelligence, Computational Entomology, Conservation Technology, Camera Traps, Insect Declines, TinyML, Biodiversity, Insects

1 Introduction

Insects are key components of all terrestrial ecosystems and comprise over half of all described animal species [1]. They are also key components of agricultural systems, essential for producing crops and feedstock sustainably, and play a major role in health, as disease vectors affecting humans and animals [2]. Declines in insect biomass and changes in diversity have received attention in recent years [3, 4, 5]. Traditional insect monitoring fieldwork methodologies — such as Pan Traps, Pitfalls, and Malaise Traps — scale poorly, due to high labour and time costs [6]. Development of scalable survey

techniques is critical for global-scale monitoring of the extent and steepness of declines [7, 6]. Technological advancements in electronics, remote cameras and artificial intelligence offer a route to meet this challenge [8, 9].

Already, camera traps have emerged as a popular method to survey populations of large mammals and birds [10]. Due to their autonomous nature, camera traps enable 24/7 monitoring across large spatial scales utilising many cameras at a low cost. The large quantities of image/video data produced by camera traps have necessitated the development of AI methods that can automatically process these data by identifying any species present in each image/video [11, 12]. Integration of camera traps and AI, handling data processing, completes an end-to-end scalable architecture suitable for fully automated, and thus globally scalable, biodiversity monitoring.

A key feature of camera traps is their trigger mechanism. Triggers, which tell the camera when to capture an image or video, must continuously operate and therefore have the largest impact on system power consumption. The specificity of the trigger (true negative rate), directly impacts the number of erroneous images saved to disk. While its recall (true positive rate) impacts the number of detections. Common fieldwork scenarios where data bandwidth and energy are limited require a low-powered, accurate trigger to enable lengthy deployments. For traditional camera traps, this is facilitated by a passive infrared (PIR) sensor which signals to record data only when sudden changes in surface temperature are detected [13] and draws very little current otherwise. Thus, camera traps can be deployed in remote locations

for months at a time, maximising the chance to observe rare or elusive species and minimising human effort.

However, PIR triggers are not appropriate for invertebrates [14], due to a lack of body heat to trigger detection. When PIR sensors have been deployed for insect studies, they are shown to have low specificity [15] and poor recall compared with scheduled image capture [16]. There are some alternatives. For example, Preti et al. surveys camera systems for integrated pest monitoring. These systems typically kill species and take time-lapsed footage to attain temporal resolution [17]. While successful, the ethics of this alternative are not appropriate to scaling conservation efforts. Other systems based on passive acoustics can be low-powered [18] and prior work has shown that utilising wing-beat harmonics can discern a modest number of species from background noise [19, 20, 21]. However, studies which are able to classify a wider range of species have invariably made use of images input into AI models [22, 23, 24, 25]. Thus, the use of camera sensors emerges as the preferred method. Non-lethal image-based systems budget power consumption poorly. For example, those filtering on-device, make use of Convolutional Neural Networks (CNNs) to improve accuracy but recommend the addition of energy harvesting to enable portability [26, 27]. The PICT system has a lower power draw and no such AI capability, but simply records continuously to disk and its deployment length is shown to be limited by storage space [28]. A recent design using event cameras for triggering is able to reduce power consumption somewhat but requires specialised hardware to do so [29].

One final challenge of image capture is trigger latency, the time between activation and image capture. This lag is nominally $<1s$ for commercial camera trap systems. Consequently, for fast-moving animals, such as flying insects, small fields of view cannot be tolerated and detection probability is diminished [30]. Methods which filter a continuous stream of images can be thought of as having zero latency, although these methods invariably require excessive power consumption for processing [31].

Here we explore how all aspects of the trigger problem may be tackled using AI executing *at the edge*. We have designed a novel trigger mechanism for insect capture, recognising (1) that image data are required to achieve high levels of species granularity; (2) that a trigger must be low-powered and accurate, and (3) that hardware platforms should be easily available and low-cost. Our method filters a continuously captured stream of images and searches for those with insect features as learned by a convolutional neural network (CNN). We are able to mitigate power consumption issues by designing our models to suit the latest power-efficient microcontroller hardware. We show how image classifiers can be trained and deployed on low-cost hardware to detect insect instances with high levels of accuracy in real-time and with zero latency. We extensively evaluate our models on validation datasets, out-of-domain examples and via analysis with saliency maps to build trust in the learned representations. We provide an early hardware implementation for an insect camera trap to quantify the power consumption and execution latency of models on-device. Our method is

found to be accurate, robust, power-efficient and fast operating on low-cost hardware.

2 Materials and Methods

The creation of a CNN model for execution on a microcontroller unit (MCU) has many challenges. So-called "TinyML" algorithms are severely constrained by the computing capability of host devices [32]. The execution memory available on the device limits model size and as MCUs typically have slow clock speeds, the latency for inference is increased, which bottlenecks processing throughput. Initially, object detection architectures seem attractive for our task, as they excel at finding small animals in images [33]. However, the number of parameters required for object detection often increases tenfold when compared to simple classifiers [34]. Thus, we take inspiration from the "Visual Wake Words" concept [35] which was shown to reliably identify human-containing images utilising a MobileNet classifier.

We elect to use the MobileNetv2 architecture as it has many built-in efficiencies [36]. We also simplify the learning problem to its most basic form, two-class (binary) classification, requesting that a single output neuron produces a value of 1.0 for insect presence in the input and 0.0 otherwise. To further save computation, our models use modest input sizes, the smallest of which is 96x96x1, as shown by Table 1. A limitation of this approach is of course resolution, which makes objects small in the image harder to detect.

In practice, this results in a reduced field of view for the deployed system, limiting its ability to detect small objects at a distance. We have also selected modest values for the α parameter, which affects the width of the network and experimented with the removal of the input colour channels which reduces the number of computations per inference. To maximise the efficiency of our models, we use a network compression technique, quantisation [37], which reduces the bit-depth of our models such that the data types representing them are more efficiently computed on MCU hardware, typically from 32-bit floating point numbers to 8-bit integers. This incurs an accuracy penalty and we monitor this throughout the evaluation.

Below are details of our method for training and evaluating these models. Specialised training and evaluation datasets for the binary insect classification task are also presented. Code for training and evaluation work was written with iterative consultation from the ChatGPT LLM, version 4o, and checked extensively by the lead author.

Model name	α	Input shape (HxWxC)	Nr. Parameters
1	0.1	(96x96x1)	94,449
2	0.1	(96x96x3)	94,593
3	0.1	(120x160x1)	94,449
4	0.1	(120x160x1)	94,593
5	0.35	(96x96x1)	411,201
6	0.35	(96x96x3)	411,489
7	0.35	(120x160x1)	411,201
8	0.35	(120x160x3)	411,489

Table 1: Model variations for binary classification, showing variations on input size and the α parameter for each model labelled 1-8. The number of model parameters as reported by Keras is shown in the rightmost column.

2.1 Datasets

Selection of an appropriate training dataset was driven by three main factors: (1) the diversity of insect species and inclusion of varied negative background examples, (2) inclusion of images of insects captured in the field to improve model transfer real-world field conditions, (3) the quantity and quality of insect images used.

We explore a variety of source datasets for insect classification and detection. The AMI-GBIF dataset, contains over 2.5 million images of 5,364 species [38], derived from the GBIF (Global Biodiversity Information Facility). Indeed the GBIF and other internet-based repositories offer many millions of images across thousands of species. While this coverage appears comprehensive, other datasets contain images of insects as they may be observed in the field [39, 27, 40] - this is critical to improve the transferability of learned representations - but they are limited by small sample sizes, featuring only a few species or images with homogenous backgrounds. To leverage both, we elected to construct a dataset comprising images from the field combined with varied examples from the iNaturalist 2017 challenge dataset [41].

We select the iNaturalist 2017 dataset due to its broad diversity encompassing 1021 insect species. We elect to use the images annotated with the 125,679 additional insect bounding boxes (hereafter referred to as “iNat2017-insecta”). This choice was made because a wide range of bounding box sizes - many of which are small - are included, making it ideal for modelling the

insect filtering task with the insect at a variety of distances from the camera. As negative samples, we also include the iNaturalist 2017 *plantae* images as this contains a variety of background foliage, referred to as “iNat2017-plantae”. Class imbalance is known to bias learned representations, thus, we carefully balance the number of background and foreground images with an equal number of examples from each data source. iNat2017-plantae images are randomly sub-sampled such that their quantity is equal to iNat2017-insecta. Images containing insects were assigned the foreground label 1 and 0 (background) otherwise.

To add field deployment data, we supplement our dataset with images captured by existing insect camera traps. We use data from Bjerge et al. [39], hereafter referred to as the “Ecostack” dataset and Sittinger et al. [27], hereafter referred to as the “Insect-Detect” dataset. The number of examples from these datasets is shown in Table 2, these make up a minority portion of the training and validation dataset; they cover 9 and 5 insect classes respectively, labels are also supplied in the bounding box format denoting the spatial location of an insect in each image.

Given the small input sizes required by our models, rescaling large, high-resolution images posed challenges as this often results in a significant loss of subject detail. Datasets, such as Ecostack and Insect-Detect contain high-resolution imagery where the insect subjects occupy only a small portion of the full frame. Full-frame down-scaling strategies for these images are not practical for use with our models. Thus, to leverage their advantages, we

preprocess each image by partitioning it into tiles, ensuring that the new resolution is a factor of 2^n , where $n \in \mathbb{N}$, relative to the original resolution. For label conversion from bounding boxes to binary classification, we assign a label of 1 to a tiled image if it contains a bounding box covering more than 50% of its area prior to tiling. Images with no overlapping bounding boxes are labelled as 0. In this process, all bounding boxes class labels are treated as the insect class, with the exception of the `shadow` class in the Insect-Detect dataset, which is treated as background. To achieve balance between the foreground and background classes a number of insect images are chosen and the background tiles are randomly sampled to equal this number or exhaust the number of unique background images.

Table 2 shows the breakdown of images in our training and validation datasets. For the validation set, examples from each dataset source’s respective validation set are used. A total of 135,451 images containing insects and 134,634 images containing backgrounds results in a train/validation ratio of 84%/16%.

Source	Insect Images (train)	Background Images (train)	Insect Images (val)	Background Images (val)
iNat2017-insecta	97524	-	16732	-
iNat2017-plantae	-	97524	-	16732
Ecostack n=2	11000	11000	1840	1840
Ecostack n=3	1981	1726	3215	2989
Insect-Detect n=2	1328	1328	190	190
Insect-Detect n=3	1456	1151	185	154
Total	113289	112729	22162	21905

Table 2: Image quantities in training and validation datasets for binary classification including breakdown of positive and negative sample quantities across iNat2017-insecta, iNat2017-plantae, Ecostack and Insect-Detect.

2.2 Training

The training was undertaken using a single Nvidia V100 GPU for each model, utilising computational resources from the JADE2 HPC facility and completed after one week of computation time.

Each model was instantiated in the Keras programming environment [42], using default implementations and hyperparameters listed in Table 1. To leverage the advantages of transfer learning, models were pre-trained for 100 epochs on the more diverse iNat2021-mini dataset with randomly initialised weights. iNat2021-mini is a variation on the iNaturalist 2021 challenge dataset which is miniaturised by reducing the number of images for each of the 10,000 classes to 10 [43]. Classes are species spread across the Tree of Life and this helps the models learn generic features for natural images. During this stage, a classification head of size 10,000 was added, which refers to the final layer responsible for mapping the learned features to the 10,000 output classes. A categorical cross-entropy loss was employed to facilitate learning. Models used the Adam optimiser [44] with default parameters from the Keras framework (fixed learning rate, $\mu = 0.001$), and training used a mini-batch size of 64 utilising the NVidia CUDA backend acceleration for TensorFlow.

Each image was resized to fit the input layer using bilinear interpolation. For greyscale images, RGB inputs were converted using the `cvtColor` function available from the OpenCV library. To help further diversify the data, a binary horizontal flip augmentation was applied with a likelihood of 50%.

Regularisation was added via a dropout layer, with an activation likelihood of 50%. This was added to the penultimate network layer, before the head [45].

After pre-training, the classification head was removed and replaced with a single output neuron for binary classification. The main training comprised a further 10 epochs on our dataset using the same method as above, except, the categorical cross-entropy loss function was replaced with binary cross-entropy. Finally, after training, each model has had its weights quantised such that they can be represented with an `int8` (signed 8-bit integer) datatype. We utilised the TensorFlow Lite for Microcontrollers software package to quantise our models [46]. Quantised variants for each model are hereafter referred to as each Q-variant.

2.3 Evaluation

We conduct a comprehensive evaluation of our models to assess their suitability as insect triggers. Initially, we compute accuracy on the withheld validation set, at a threshold of 50%, as reported by Keras. While a useful measure, it does not recognise that different use cases may set a threshold for detection based on the user preference for specificity or recall. Thus, we utilise receiver operating characteristic (ROC) curves to explore the process of thresholding the ordinal scale output of each model into binary predictions. This allows us to explore the trade-off between recall and specificity at various thresholds. We distil ROC performance to a single value, the area under

the curve (AUC) [47], appropriately capturing overall performance across all thresholds and allowing models to be easily compared across various configurations and datasets. A model with a 1.0 AUC value is perfect, one with 0.5 has no discriminative power and one with an AUC value of 0.0 perfectly miss-labels all examples at all thresholds.

Using this mode of comparison, we explore how our models adapt to deployment-style datasets which are unseen and seen during training. We compute the AUC for both the Ecostack and Insect-Detect datasets and for two datasets of deployment-style data unseen in training. We choose Bjerge et al. [40]’s dataset of pollinator images (hereafter referred to as Pollinator-Detect) and the camera trap images from the AMI Dataset (hereafter referred to as AMI-CT) [38]. These data are tiled in the same manner outlined in Section 2.1 resulting in a binary classification dataset of field deployment data for a realistic test of performance.

Next, we investigate the legitimacy of the features learned by the model. A common problem in supervised learning is over-fitting to characteristics of the training data which do not generalise to new domains. For example Schneider et al. found classification performance to drastically reduce when the same animal is shown with different backgrounds [48]. To build trust in learned features, we endeavour to determine the most impactful image regions using saliency maps. Saliency maps graphically show the output gradient with respect to the input image, indicating how sensitive the model’s prediction is to changes in each pixel. We make use of the bounding box labels

previously discarded in training to quantify the intersection of salient areas and the corresponding area of the image containing an insect. Figure 1 shows our workflow simplified.

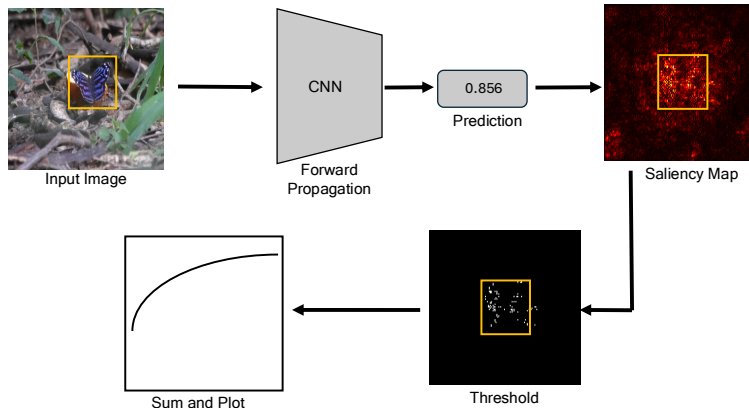


Figure 1: Simplified workflow for saliency map analysis showing the main stages. Inference yields a prediction and a corresponding saliency map, salient pixels are thresholded, creating a binary map. Pixels within the insect bounding box are counted and the portion of salient pixels is plotted for all thresholds and images.

While there are many methods for computing saliency maps [49]. We opt for “Vanilla Gradient” for simplicity. This computes the gradient of the output per pixel. As we only have a single output neuron representing both classes, we consider positive gradients only as those corresponding to insects. Equation 1 shows this, where $S_{i,j}$ is the saliency map, $I_{i,j}$ is the input image and y is the output prediction.

$$S_{i,j}^k = \max \left(0, \frac{\partial y}{\partial I_{i,j}^k} \right) \quad (1)$$

The integer, $k \in \mathbb{N}$ denotes the index of each input image. Each saliency map is also normalised, such that its dynamic range lies within $[0.0, 1.0]$. Saliency maps are then binarised for each threshold, $t \in [0.0, 1.0]$:

$$S_{i,j}^{k,t} = \begin{cases} 1, & \text{if } S_{i,j}^k \geq t, \\ 0, & \text{if } S_{i,j}^k < t \end{cases} \quad (2)$$

e number of pixels within $S_{i,j}^{k,t}$ which lie within any bounding box range within the k^{th} image. Thus compute \bar{P}^t as the average P_k^t over all k as shown by Equation 3. We repeat this for all models and \bar{P} plotted over all values of t to provide a visualisation of model performance. As the value of t rises, \bar{P} is expected to rise, indicating that the most salient pixels consistently lie within the image portion containing an insect. The area under this curve and maximum \bar{P}_t reflects the robustness of the learned saliency maps.

$$\bar{P}^t = \frac{1}{N} \sum_{k=1}^N P_k^t \quad (3)$$

Finally, minimisation of power consumption has been a key driver for the design decisions taken throughout this work and thus forms the final component of our analysis. To measure power consumption, we select a deployment platform, compile our models and execute them on the device. MCU code is written to target the ESP32-S3 chipset. We chose this platform as it is low-cost, readily available and supports the ESP-NN neural network acceleration library to speed up inference time, which boosts system throughput.

ESP-NN (available at: <https://github.com/espressif/esp-nn>) is a C++ library supported by the chip manufacturer, Espressive. It provides optimised neural network execution functions which are between 3 and 10 times faster than vanilla operations; in our firmware, we use version 1.0. We also use the LILYGO® T-SIMCAM ESP32-S3 Development Board as a target, although similar development boards would suffice. These are available for a retail price of around £20, including an embedded camera, wireless connectivity and the capacity to hold an SD and SIM card.

Our testing firmware is very simple, images are captured at a resolution equal to the input size of the network, then, inference is then executed using the TensorFlow Lite Micro runtime and this process is timed. We measure the time taken for inference and average over five inferences for each model. Current consumption is measured using a desk ammeter while idle and while running our programme. The system is powered using a bench power supply set to 3.3V.

3 Results

The validation accuracy and AUC values for each model variant are summarised in Table 3, and ROC curves are presented in Figure 2. Further testing utilised the Insect-Detect, Ecostack, Pollinator-Detect and AMI-CT data with the tiling parameter, n , set to 2. Across all models, validation accuracy ranges from 0.836 to 0.904, indicating a strong overall performance. This

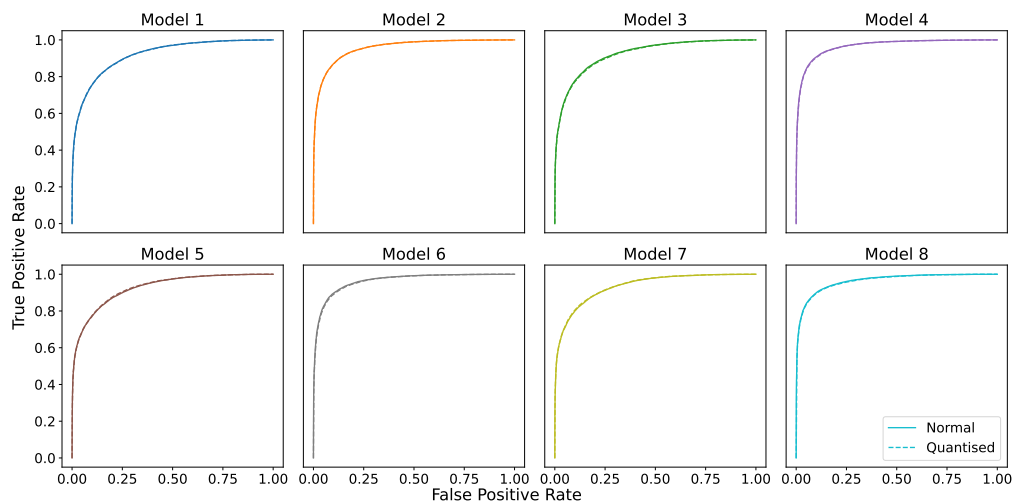


Figure 2: ROC curves for each model computed from the validation dataset. Quantised models shown as dotted lines, while solid lines show each original, unquantised model

trend is consistent across output thresholds, with validation AUC ranging from 0.918 to 0.964. Strong performance is extended to the Q-variants with very modest reductions in AUC values, illustrating that quantisation does not significantly degrade the performance. On the other hand, the colourblind models generally underperform compared to models utilising RGB inputs. This trend is particularly evident for the more challenging Pollinator-Detect dataset, where AUC values fall considerably.

On the field datasets, model performance is mixed. The Pollinator-Detect dataset proved the most challenging to learn across all models and performance for the smaller models is especially weak in these examples. Performance on Insect-Detect and Ecostack is strong and consistently outperforms validation. On the AMI-CT dataset, out-of-domain performance remains

strong. These results suggest our models have high discriminative power when insects appear on simple, uncluttered backgrounds or when data are from the same distribution as the training source.

Model	Val. Accuracy	Val. AUC	Insect-Detect AUC n=2	Ecostack AUC n=2	Pollinator-Detect AUC n=2	AMI-CT AUC n=2
1	0.836	0.918	0.955	0.840	0.635	0.818
(Q-variant)		(0.918)	(0.952)	(0.838)	(0.637)	(0.818)
2	0.883	0.955	0.959	0.887	0.588	0.841
(Q-variant)		(0.955)	(0.959)	(0.887)	(0.594)	(0.836)
3	0.817	0.923	0.970	0.841	0.605	0.854
(Q-variant)		(0.921)	(0.970)	(0.829)	(0.604)	(0.856)
4	0.900	0.966	0.972	0.941	0.637	0.859
(Q-variant)		(0.965)	(0.971)	(0.937)	(0.644)	(0.856)
5	0.844	0.925	0.976	0.868	0.595	0.859
(Q-variant)		(0.927)	(0.974)	(0.871)	(0.608)	(0.860)
6	0.896	0.963	0.974	0.932	0.691	0.835
(Q-variant)		(0.961)	(0.970)	(0.924)	(0.700)	(0.827)
7	0.857	0.934	0.982	0.866	0.600	0.860
(Q-variant)		(0.935)	(0.981)	(0.867)	(0.596)	(0.861)
8	0.904	0.964	0.992	0.959	0.680	0.872
(Q-variant)		(0.961)	(0.991)	(0.957)	(0.674)	(0.869)

Table 3: Table of numerical results for each model showing validation accuracy after 10 epochs and area under the ROC curve for respective datasets. Additional validation accuracy and validation AUC is given for each model post-quantisation.

Curves for our saliency map analysis are presented in Figure 2. Some examples of saliency map predictions are shown for in-domain data in Figure 5 and for out-of-domain data in Figure 6. These curves reveal a consistent pattern with the accuracy analysis, the colourblind models display a more fragile learned representation, as evidenced by a low proportion of salient pixels within insect bounding boxes. In contrast, the RGB models consistently show that the most salient pixels lie in areas of the images belonging to insects, suggesting a more robust learned representation which can be more easily generalised.

Power consumption and inference latency characteristics of each model

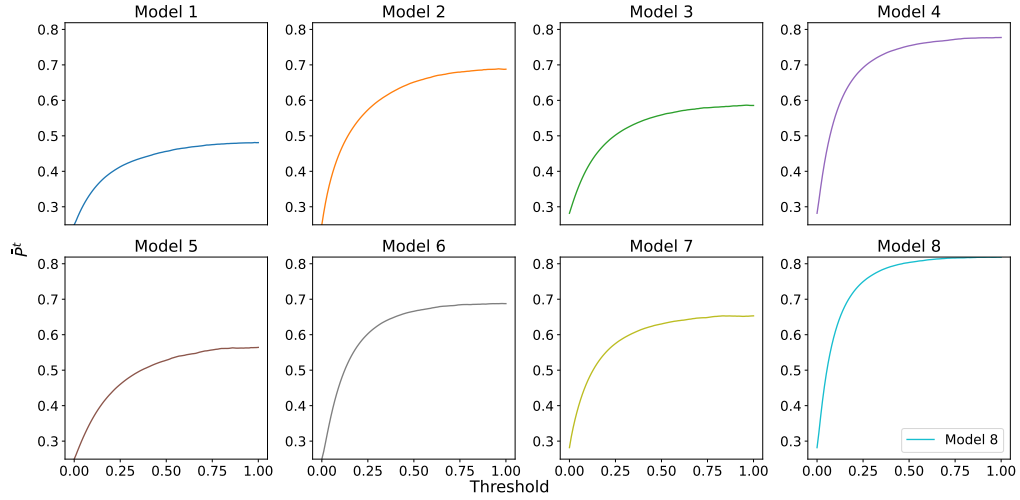


Figure 3: Resultant curves for \bar{P}^t for each model as computed on the validation dataset.

are shown in Figure 4. This also shows how the number of frames-per-second processed by the system can affect power consumption as this defines the proportion of time the MCU executes instructions vs the proportion of time it is sitting idle. Operating at their highest throughput, all models consume less than 300mW and at half throughput this can be reduced to around 185mW. The most lightweight models, 1 and 2, can process over eight frames per second. The most accurate model, 8, can process over two frames per second.

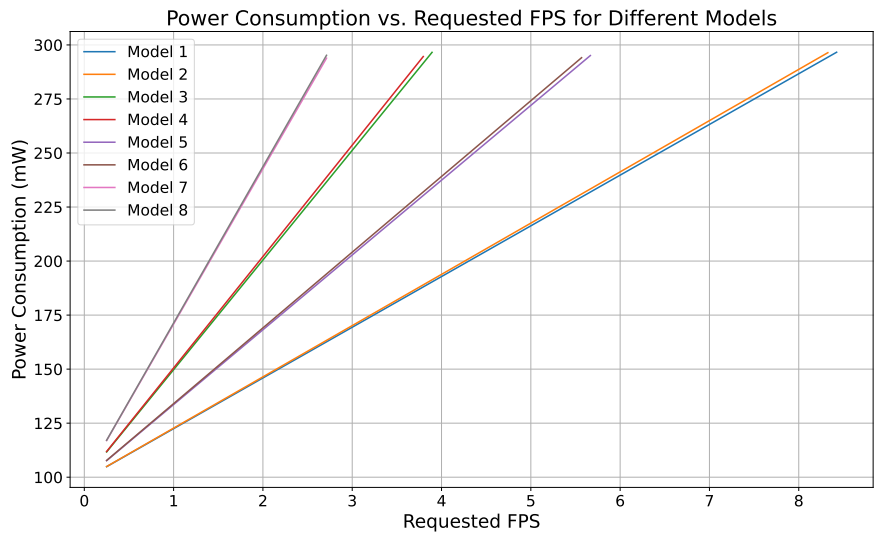


Figure 4: Average power consumption for each model versus operational frames per second processed by the ESP32-S3 chipset.

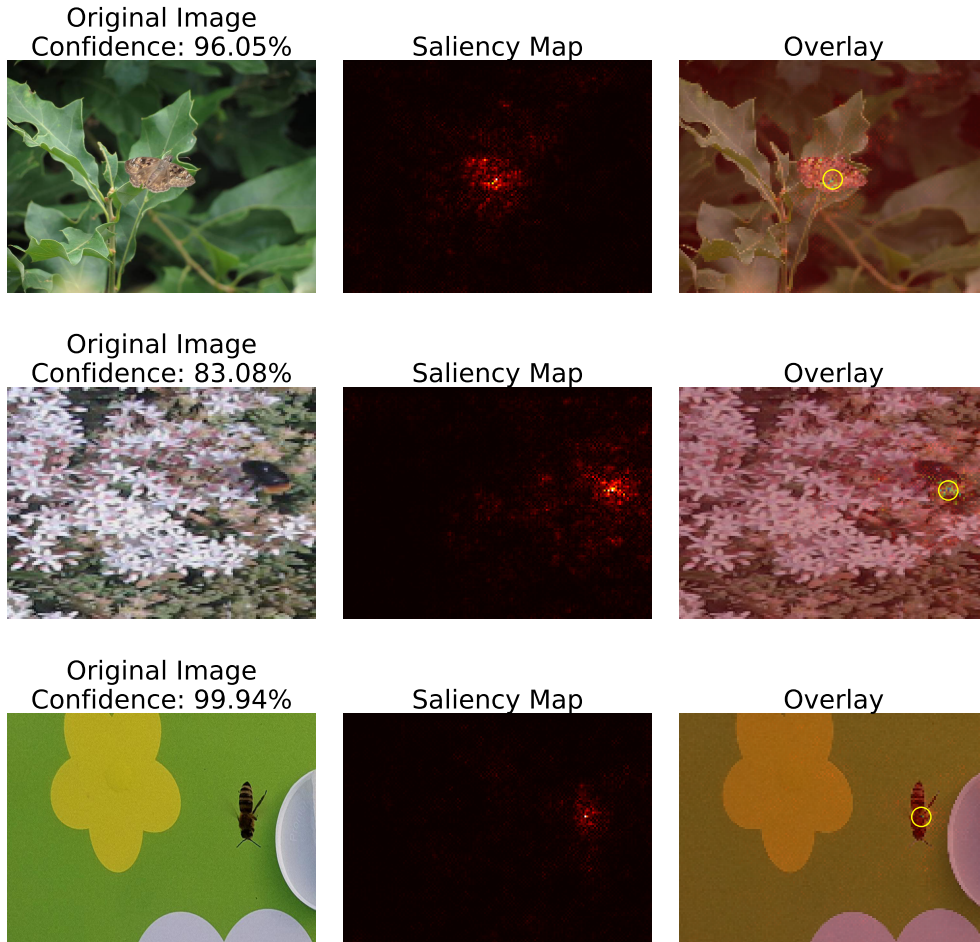


Figure 5: Example predictions from our validation dataset, executed using model 8. Input images with their prediction confidence are shown in the leftmost column, saliency maps are shown in the center column and the rightmost column overlays this with the input image. In the rightmost column, the most salient pixel is highlighted with an encompassing circle.



Figure 6: Example predictions from datasets unseen in training, executed using model 8. Input images with their prediction confidence are shown in the leftmost column, saliency maps are shown in the centre column and the rightmost column overlays this with the input image. In the rightmost column, the most salient pixel is highlighted with an encompassing circle. The first row includes an insect image from Pollinator-Detect. The second row is of a sticky trap image from [50]. The final row is of an AMI-CT image.

4 Discussion

Our results have revealed our models to be excellent candidates for insect camera trap trigger mechanisms. They achieved high accuracy while specificity and recall rates remained robust across output thresholds - even when tested on out-of-domain datasets. Furthermore, saliency map analysis provided insights into the reliability of the learned features, with RGB models consistently focusing on insect-related image regions, reinforcing trust in their generalisation capacity. Our approach also achieved significant reductions in power consumption when deployed on low-powered microcontroller hardware.

Our saliency map analysis has given critical insights. Colourblind models have demonstrated a tendency to rely on background information rather than the insect features themselves, as demonstrated by the low proportion of salient pixels in foreground regions. The drop in \bar{P}_t is much more serious than a simple drop in accuracy as a brittle learned representation has likely overfit to the training data. In contrast, the RGB models demonstrated that most salient pixels are located in the foreground, increasing confidence in these models and also serving as a warning that some background correlations have likely been learned throughout the training.

Our system’s reduced power consumption presents several use cases, primarily in scenarios where energy harvesting is not viable, such as beneath jungle canopies or in other shaded or confined environments such as treetops.

The PICT system, a widely cited example, consumes 0.76W during daytime, which allows it to run for 146 hours on a 111 Wh battery. However, with a 64GB SD card, the storage fills up after just three days of recording. The system has a high rate of false positive recordings — during a trial, 1147 hours of footage were recorded, 95% of which did not capture motion attributed to insect presence, as there was no on-device filtering. In contrast, our system consumes less than half the power of PICT, operating at full frame rate with just 300mW, extending battery life to 370 hours — equivalent to a month’s worth of 12-hour daytime periods. Reducing the framerate by half further extends battery life to approximately 600 hours, a massive performance gain. Moreover, the improved specificity of our models will significantly increase the deployment period of an SD card. If just 80% of false positive frames were removed from PICT, 76% of trial hours would have been saved. Per SD card this would extend deployment periods to over 12 days.

Beyond long-term deployments, our system has potential when used as an external trigger for applications where real-time, low-latency triggers are critical, such as plant-pollinator interaction monitoring. In these cases, where insects remain stationary for a period, our camera trap could act as an external trigger for high-resolution cameras, improving data quality while maintaining low energy consumption overall. This is a step-change in how ectotherms are sensed in the field and may drastically improve poor specificity of pollination ecology studies [15].

One benefit of edge intelligence is the ability to autonomously make de-

cisions based on what data are interpreted on the fly [51]. Our method facilitates flexible sampling routines, power consumption could be dynamically budgeted based on environmental conditions or real-time data interpretation. Sampling rates may be increased when insect activity is detected while operating at lower rates during periods of inactivity to conserve energy.

While promising, this method has several limitations that can be explored in future work. Power consumption is markedly lower than similar systems, but can be reduced much further in the idle state by utilising further firmware engineering aspects such as utilising MCU sleep modes which may drastically reduce power consumption between model inferences or during system downtimes. Our models have also encountered challenges in generalising to the challenging out-of-domain Pollinator-Detect dataset, suggesting they require refinements for some downstream use cases. This could be addressed in the selection of training data, as more field datasets become available, domain shift size may diminish, allowing higher accuracy scores. The method we have shown allows further training data to be integrated easily, improving flexibility. The low input resolution of our models limits their field of view, this constraint was required by the compute capability of MCU hardware. Recent innovations in lightweight, shallow convolutional networks may provide larger input sizes within the same compute budget [52]. This may allow for higher-resolution imagery to be processed improving detection of small insects in-frame. The framerate throughput of our MCU deployment example is considerably lower than competing systems which record video

continuously. This constraint is required by the execution latency of our models but can be corrected in several ways. Riechmann et al. [31] showcase an algorithm to budget inferences across continuous frames and attain a large speedup. Further, model latency could be reduced by using additional compression methods such as network pruning [53].

Finally, while in this work we focus on addressing insect monitoring, these concepts could be applied to the retrieval of animal images more generally. Meek and Pittet found that faster trigger times are one of the most common requests from conventional camera trap users [54] and PIR sensors have been shown to generate many false triggers, for example, the Snapshot Serengeti camera trap trail data contains over 1.2 million images and only 26% were found to contain animals [55]. Our method, with zero latency, and high accuracy provides new directions. This method as a replacement for, or working alongside, PIR triggers in traditional camera traps may help to address low recall of fast-moving small animals and address the large number of false positive triggered images.

5 Conclusion

Using the latest innovations in MCU hardware and lightweight supervised learning, we have shown how insect monitoring can be made scalable by solving the challenging trigger problem. Through extensive analysis, we have established trust in our methods, proving that our models are well-suited for

this purpose. Our early hardware implementation is also novel and saves energy and cost using readily available components.

This method has the potential to transform non-invasive insect monitoring in the future. Our solution is scalable, providing a step-change in capability, allowing systems to be deployed in greater quantity, improving sampling density and scale without the need for excessive manual labour. Such tools are essential for the timely assessment of biodiversity trends in the wake of current environmental uncertainties.

References

- [1] Nigel E. Stork. How many species of insects and other terrestrial arthropods are there on earth? *Annual Review of Entomology*, 63(Volume 63, 2018):31–45, 2018. ISSN 1545-4487. doi: <https://doi.org/10.1146/annurev-ento-020117-043348>. URL <https://www.annualreviews.org/content/journals/10.1146/annurev-ento-020117-043348>.
- [2] Duane J Gubler. The global emergence/resurgence of arboviral diseases as public health problems. *Archives of Medical Research*, 33(4):330–342, 2002. ISSN 0188-4409. doi: [https://doi.org/10.1016/S0188-4409\(02\)00378-8](https://doi.org/10.1016/S0188-4409(02)00378-8). URL <https://www.sciencedirect.com/science/article/pii/S0188440902003788>.
- [3] Roel van Klink, Diana E. Bowler, Konstantin B. Gongalsky, Ann B.

- Swengel, Alessandro Gentile, and Jonathan M. Chase. Meta-analysis reveals declines in terrestrial but increases in freshwater insect abundances. *Science*, 368(6489):417–420, 2020. doi: 10.1126/science.aax9931. URL <https://www.science.org/doi/abs/10.1126/science.aax9931>.
- [4] David L. Wagner, Eliza M. Grames, Matthew L. Forister, May R. Berenbaum, and David Stopak. Insect decline in the anthropocene: Death by a thousand cuts. *Proceedings of the National Academy of Sciences*, 118(2):e2023989118, 2021. doi: 10.1073/pnas.2023989118. URL <https://www.pnas.org/doi/abs/10.1073/pnas.2023989118>.
- [5] Caspar A. Hallmann, Martin Sorg, Eelke Jongejans, Henk Siepel, Nick Hofland, Heinz Schwan, Werner Stenmans, Andreas Müller, Hubert Sumser, Thomas Hörren, Dave Goulson, and Hans de Kroon. More than 75 percent decline over 27 years in total flying insect biomass in protected areas. *PLOS ONE*, 12(10):1–21, 10 2017. doi: 10.1371/journal.pone.0185809. URL <https://doi.org/10.1371/journal.pone.0185809>.
- [6] Graham A. Montgomery, Michael W. Belitz, Rob P. Guralnick, and Morgan W. Tingley. Standards and best practices for monitoring and benchmarking insects. *Frontiers in Ecology and Evolution*, 8, 2021. ISSN 2296-701X. doi: 10.3389/fevo.2020.579193. URL <https://www.frontiersin.org/journals/ecology-and-evolution/articles/10.3389/fevo.2020.579193>.
- [7] Rudolf Meier, Emily Hartop, Christian Pylatiuk, and Amrita Srivath-

- san. Towards holistic insect monitoring: species discovery, description, identification and traits for all insects. *Philosophical Transactions of the Royal Society B: Biological Sciences*, 379(1904):20230120, 2024. doi: 10.1098/rstb.2023.0120. URL <https://royalsocietypublishing.org/doi/abs/10.1098/rstb.2023.0120>.
- [8] Barbara A. Han, Kush R. Varshney, Shannon LaDeau, Ajit Subramaniam, Kathleen C. Weathers, and Jacob Zwart. A synergistic future for ai and ecology. *Proceedings of the National Academy of Sciences*, 120(38):e2220283120, 2023. doi: 10.1073/pnas.2220283120. URL <https://www.pnas.org/doi/abs/10.1073/pnas.2220283120>.
- [9] Toke T. Høye, Johanna Ärje, Kim Bjerger, Oskar L. P. Hansen, Alexandros Iosifidis, Florian Leese, Hjalte M. R. Mann, Kristian Meissner, Claus Melvad, and Jenni Raitoharju. Deep learning and computer vision will transform entomology. *Proceedings of the National Academy of Sciences*, 118(2):e2002545117, 2021. doi: 10.1073/pnas.2002545117. URL <https://www.pnas.org/doi/abs/10.1073/pnas.2002545117>.
- [10] Robin Steenweg, Mark Hebblewhite, Roland Kays, Jorge Ahumada, Jason T Fisher, Cole Burton, Susan E Townsend, Chris Carbone, J Marcus Rowcliffe, Jesse Whittington, Jedediah Brodie, J Andrew Royle, Adam Switalski, Anthony P Clevenger, Nicole Heim, and Lindsey N Rich. Scaling-up camera traps: monitoring the planet’s biodiversity with networks of remote sensors. *Frontiers in Ecology and*

- the Environment*, 15(1):26–34, 2017. doi: <https://doi.org/10.1002/fee.1448>. URL <https://esajournals.onlinelibrary.wiley.com/doi/abs/10.1002/fee.1448>.
- [11] Mohammad Sadegh Norouzzadeh, Anh Nguyen, Margaret Kosmala, Alexandra Swanson, Meredith S. Palmer, Craig Packer, and Jeff Clune. Automatically identifying, counting, and describing wild animals in camera-trap images with deep learning. *Proceedings of the National Academy of Sciences*, 115(25):E5716–E5725, 2018. doi: 10.1073/pnas.1719367115. URL <https://www.pnas.org/doi/abs/10.1073/pnas.1719367115>.
- [12] Robin C. Whytock, Jędrzej Świeżewski, Joeri A. Zwerts, Tadeusz Bara-Słupski, Aurélie Flore Koumba Pambo, Marek Rogala, Laila Bahaa-el din, Kelly Boekee, Stephanie Brittain, Anabelle W. Cardoso, Philipp Henschel, David Lehmann, Brice Momboua, Cisquet Kiebou Opepa, Christopher Orbell, Ross T. Pitman, Hugh S. Robinson, and Katharine A. Abernethy. Robust ecological analysis of camera trap data labelled by a machine learning model. *Methods in Ecology and Evolution*, 12(6):1080–1092, 2021. doi: <https://doi.org/10.1111/2041-210X.13576>. URL <https://besjournals.onlinelibrary.wiley.com/doi/abs/10.1111/2041-210X.13576>.
- [13] Dustin J. Welbourne, Andrew W. Claridge, David J. Paull, and Andrew Lambert. How do passive infrared triggered camera traps oper-

- ate and why does it matter? breaking down common misconceptions. *Remote Sensing in Ecology and Conservation*, 2(2):77–83, 2016. doi: <https://doi.org/10.1002/rse2.20>. URL <https://zslpublications.onlinelibrary.wiley.com/doi/abs/10.1002/rse2.20>.
- [14] Michael T. Hobbs and Cheryl S. Brehme. An improved camera trap for amphibians, reptiles, small mammals, and large invertebrates. *PLOS ONE*, 12(10):1–15, 10 2017. doi: 10.1371/journal.pone.0185026. URL <https://doi.org/10.1371/journal.pone.0185026>.
- [15] Peter R. Houlihan, Mac Stone, Shawn E. Clem, Mike Owen, and Thomas C. Emmel. Pollination ecology of the ghost orchid (*Dendrophylax lindenii*): A first description with new hypotheses for darwin’s orchids. *Scientific Reports*, 9(1):12850, 2019. ISSN 2045-2322. doi: 10.1038/s41598-019-49387-4. URL <https://doi.org/10.1038/s41598-019-49387-4>.
- [16] Qaim Naqvi, Patrick J. Wolff, Brenda Molano-Flores, and Jinelle H. Sperry. Camera traps are an effective tool for monitoring insect–plant interactions. *Ecology and Evolution*, 12(6):e8962, 2022. doi: <https://doi.org/10.1002/ece3.8962>. URL <https://onlinelibrary.wiley.com/doi/abs/10.1002/ece3.8962>.
- [17] Michele Preti, François Verheggen, and Sergio Angeli. Insect pest monitoring with camera-equipped traps: strengths and limitations.

- Journal of Pest Science*, 94(2):203–217, 2021. ISSN 1612-4766.
doi: 10.1007/s10340-020-01309-4. URL <https://doi.org/10.1007/s10340-020-01309-4>.
- [18] Paolo Volponi, Leonardo Dapporto, and Marta Skowron Volponi. The buzzometer system: In situ audio recordings of pollinators in flight. *Methods in Ecology and Evolution*, 14(12):2985–2993, 2023. doi: <https://doi.org/10.1111/2041-210X.14224>. URL <https://besjournals.onlinelibrary.wiley.com/doi/abs/10.1111/2041-210X.14224>.
- [19] Topu Saha, Adrien P. Genoud, Gregory M. Williams, and Benjamin P. Thomas. Monitoring the abundance of flying insects and atmospheric conditions during a 9-month campaign using an entomological optical sensor. *Scientific Reports*, 13(1):15606, 2023. ISSN 2045-2322. doi: 10.1038/s41598-023-42884-7. URL <https://doi.org/10.1038/s41598-023-42884-7>.
- [20] Satoshi Kawakita and Kotaro Ichikawa. Automated classification of bees and hornet using acoustic analysis of their flight sounds. *Apidologie*, 50(1):71–79, February 2019. ISSN 1297-9678. doi: 10.1007/s13592-018-0619-6. URL <https://doi.org/10.1007/s13592-018-0619-6>.
- [21] Ivan Kiskin, Davide Zilli, Yunpeng Li, Marianne Sinka, Kathy Willis, and Stephen Roberts. Bioacoustic detection with wavelet-conditioned convolutional neural networks. *Neural Computing*

- and Applications*, 32(4):915–927, February 2020. ISSN 1433-3058. doi: 10.1007/s00521-018-3626-7. URL <https://doi.org/10.1007/s00521-018-3626-7>.
- [22] Samuel Stevens, Jiaman Wu, Matthew J Thompson, Elizabeth G Campolongo, Chan Hee Song, David Edward Carlyn, Li Dong, Wasila M Dahdul, Charles Stewart, Tanya Berger-Wolf, et al. Bioclip: A vision foundation model for the tree of life. In *Proceedings of the IEEE/CVF Conference on Computer Vision and Pattern Recognition*, pages 19412–19424, 2024.
- [23] Hoang-Quan Nguyen, Thanh-Dat Truong, Xuan Bac Nguyen, Ashley Dowling, Xin Li, and Khoa Luu. Insect-foundation: A foundation model and large-scale 1m dataset for visual insect understanding. In *Proceedings of the IEEE/CVF Conference on Computer Vision and Pattern Recognition*, pages 21945–21955, 2024.
- [24] Kim Bjerge, Quentin Geissmann, Jamie Alison, Hjalte M.R. Mann, Toke T. Høye, Mads Dyrmann, and Henrik Karstoft. Hierarchical classification of insects with multitask learning and anomaly detection. *Ecological Informatics*, 77:102278, 2023. ISSN 1574-9541. doi: <https://doi.org/10.1016/j.ecoinf.2023.102278>. URL <https://www.sciencedirect.com/science/article/pii/S1574954123003072>.
- [25] J. Christopher D. Terry, Helen E. Roy, and Tom A. August. Thinking like a naturalist: Enhancing computer vision of citizen science

- images by harnessing contextual data. *Methods in Ecology and Evolution*, 11(2):303–315, 2020. doi: <https://doi.org/10.1111/2041-210X.13335>. URL <https://besjournals.onlinelibrary.wiley.com/doi/abs/10.1111/2041-210X.13335>.
- [26] Kim Bjerge, Jakob Bonde Nielsen, Martin Videbæk Sepstrup, Flemming Helsing-Nielsen, and Toke Thomas Høye. An automated light trap to monitor moths (lepidoptera) using computer vision-based tracking and deep learning. *Sensors*, 21(2), 2021. ISSN 1424-8220. doi: 10.3390/s21020343. URL <https://www.mdpi.com/1424-8220/21/2/343>.
- [27] Maximilian Sittinger, Johannes Uhler, Maximilian Pink, and Annette Herz. Insect detect: An open-source diy camera trap for automated insect monitoring. *PLOS ONE*, 19(4):1–28, 04 2024. doi: 10.1371/journal.pone.0295474. URL <https://doi.org/10.1371/journal.pone.0295474>.
- [28] Vincent Droissart, Laura Azandi, Eric Rostand Onguene, Marie Savignac, Thomas B. Smith, and Vincent Deblauwe. Pict: A low-cost, modular, open-source camera trap system to study plant–insect interactions. *Methods in Ecology and Evolution*, 12(8):1389–1396, 2021. doi: <https://doi.org/10.1111/2041-210X.13618>. URL <https://besjournals.onlinelibrary.wiley.com/doi/abs/10.1111/2041-210X.13618>.
- [29] Eike Gebauer, Sebastian Thiele, Pierre Ouvrard, Adrien Sicard, and Benjamin Risse. Towards a dynamic vision sensor-based insect camera

- trap. In *Proceedings of the IEEE/CVF Winter Conference on Applications of Computer Vision*, pages 7157–7166, 2024.
- [30] Paul Glover-Kapfer, Carolina A. Soto-Navarro, and Oliver R. Wearn. Camera-trapping version 3.0: current constraints and future priorities for development. *Remote Sensing in Ecology and Conservation*, 5(3):209–223, 2019. doi: <https://doi.org/10.1002/rse2.106>. URL <https://zslpublications.onlinelibrary.wiley.com/doi/abs/10.1002/rse2.106>.
- [31] Miklas Riechmann, Ross Gardiner, Kai Waddington, Ryan Rueger, Frederic Fol Leymarie, and Stefan Rueger. Motion vectors and deep neural networks for video camera traps. *Ecological Informatics*, 69:101657, 2022. ISSN 1574-9541. doi: <https://doi.org/10.1016/j.ecoinf.2022.101657>. URL <https://www.sciencedirect.com/science/article/pii/S1574954122001066>.
- [32] Rakhee Kallimani, Krishna Pai, Prasoon Raghuvanshi, Sridhar Iyer, and Onel LA López. Tinyml: Tools, applications, challenges, and future research directions. *Multimedia Tools and Applications*, 83(10):29015–29045, 2024.
- [33] Fagner Cunha, Eulanda M. dos Santos, Raimundo Barreto, and Juan G. Colonna. Filtering empty camera trap images in embedded systems. In *Proceedings of the IEEE/CVF Conference on Computer Vision and Pattern Recognition (CVPR) Workshops*, pages 2438–2446, June 2021.

- [34] Andrew G. Howard, Menglong Zhu, Bo Chen, Dmitry Kalenichenko, Weijun Wang, Tobias Weyand, Marco Andreetto, and Hartwig Adam. Mobilenets: Efficient convolutional neural networks for mobile vision applications. *CoRR*, abs/1704.04861, 2017. URL <http://arxiv.org/abs/1704.04861>.
- [35] Aakanksha Chowdhery, Pete Warden, Jonathon Shlens, Andrew Howard, and Rocky Rhodes. Visual wake words dataset, 2019. URL <https://arxiv.org/abs/1906.05721>.
- [36] Mark Sandler, Andrew Howard, Menglong Zhu, Andrey Zhmoginov, and Liang-Chieh Chen. Mobilenetv2: Inverted residuals and linear bottlenecks. In *Proceedings of the IEEE conference on computer vision and pattern recognition*, pages 4510–4520, 2018.
- [37] Benoit Jacob, Skirmantas Kligys, Bo Chen, Menglong Zhu, Matthew Tang, Andrew G. Howard, Hartwig Adam, and Dmitry Kalenichenko. Quantization and training of neural networks for efficient integer-arithmetic-only inference. *CoRR*, abs/1712.05877, 2017. URL <http://arxiv.org/abs/1712.05877>.
- [38] Aditya Jain, Fagner Cunha, Michael James Bunsen, Juan Sebastián Cañas, Léonard Pasi, Nathan Pinoy, Flemming Helsing, JoAnne Russo, Marc Botham, Michael Sabourin, Jonathan Frechette, Alexandre Anctil, Yacksecari Lopez, Eduardo Navarro, Filonila Perez Pimentel, Ana Cecilia Zamora, José Alejandro Ramirez Silva, Jonathan Gagnon, Tom

August, Kim Bjerger, Alba Gomez Segura, Marc Bélisle, Yves Basset, Kent P. McFarland, David Roy, Toke Thomas Høye, Maxim Larrivé, and David Rolnick. Insect identification in the wild: The ami dataset, May 2024. URL <https://doi.org/10.5281/zenodo.11358689>.

[39] Kim Bjerger, Jamie Alison, Mads Dyrmann, Carsten Eie Frigaard, Hjalte M. R. Mann, and Toke Thomas Høye. Accurate detection and identification of insects from camera trap images with deep learning. *PLOS Sustainability and Transformation*, 2(3):1–18, 03 2023. doi: 10.1371/journal.pstr.0000051. URL <https://doi.org/10.1371/journal.pstr.0000051>.

[40] Kim Bjerger, Carsten Eie Frigaard, and Henrik Karstoft. Object detection of small insects in time-lapse camera recordings. *Sensors*, 23(16), 2023. ISSN 1424-8220. doi: 10.3390/s23167242. URL <https://www.mdpi.com/1424-8220/23/16/7242>.

[41] Grant Van Horn, Oisin Mac Aodha, Yang Song, Yin Cui, Chen Sun, Alex Shepard, Hartwig Adam, Pietro Perona, and Serge Belongie. The inaturalist species classification and detection dataset. In *Proceedings of the IEEE conference on computer vision and pattern recognition*, pages 8769–8778, 2018.

[42] François Chollet et al. Keras. <https://keras.io>, 2015.

[43] Grant Van Horn, Elijah Cole, Sara Beery, Kimberly Wilber, Serge Be-

- longie, and Oisín Mac Aodha. Benchmarking representation learning for natural world image collections, 2021. URL <https://arxiv.org/abs/2103.16483>.
- [44] Diederik Kingma and Jimmy Ba. Adam: A method for stochastic optimization. In *International Conference on Learning Representations (ICLR)*, San Diego, CA, USA, 2015.
- [45] Nitish Srivastava, Geoffrey Hinton, Alex Krizhevsky, Ilya Sutskever, and Ruslan Salakhutdinov. Dropout: A simple way to prevent neural networks from overfitting. *Journal of Machine Learning Research*, 15(56):1929–1958, 2014. URL <http://jmlr.org/papers/v15/srivastava14a.html>.
- [46] Robert David, Jared Duke, Advait Jain, Vijay Janapa Reddi, Nat Jeffries, Jian Li, Nick Kreeger, Ian Nappier, Meghna Natraj, Shlomi Regev, Rocky Rhodes, Tiezhen Wang, and Pete Warden. Tensorflow lite micro: Embedded machine learning on tinymml systems. *CoRR*, abs/2010.08678, 2020. URL <https://arxiv.org/abs/2010.08678>.
- [47] Jayawant N. Mandrekar. Receiver operating characteristic curve in diagnostic test assessment. *Journal of Thoracic Oncology*, 5(9):1315–1316, 2010. ISSN 1556-0864. doi: <https://doi.org/10.1097/JTO.0b013e3181ec173d>. URL <https://www.sciencedirect.com/science/article/pii/S1556086415306043>.

- [48] Stefan Schneider, Saul Greenberg, Graham W. Taylor, and Stefan C. Kremer. Three critical factors affecting automated image species recognition performance for camera traps. *Ecology and Evolution*, 10(7): 3503–3517, 2020. doi: <https://doi.org/10.1002/ece3.6147>. URL <https://onlinelibrary.wiley.com/doi/abs/10.1002/ece3.6147>.
- [49] Christoph Molnar. *Interpretable Machine Learning*. 2 edition, 2022. URL <https://christophm.github.io/interpretable-ml-book>.
- [50] Song-Quan Ong and Toke Thomas Høye. An annotated image dataset of pests on different coloured sticky traps acquired with different imaging devices. *Data in Brief*, 55:110741, 2024. ISSN 2352-3409. doi: <https://doi.org/10.1016/j.dib.2024.110741>. URL <https://www.sciencedirect.com/science/article/pii/S235234092400708X>.
- [51] D. B. Roy, J. Alison, T. A. August, M. Bélisle, K. Bjerger, J. J. Bowden, M. J. Bunsen, F. Cunha, Q. Geissmann, K. Goldmann, A. Gomez-Segura, A. Jain, C. Huijbers, M. Larrivière, J. L. Lawson, H. M. Mann, M. J. Mazerolle, K. P. McFarland, L. Pasi, S. Peters, N. Pinoy, D. Rolnick, G. L. Skinner, O. T. Strickson, A. Svenning, S. Teagle, and T. T. Høye. Towards a standardized framework for ai-assisted, image-based monitoring of nocturnal insects. *Philosophical Transactions of the Royal Society B: Biological Sciences*, 379(1904):20230108, 2024. doi: 10.1098/rstb.2023.0108. URL <https://royalsocietypublishing.org/doi/abs/10.1098/rstb.2023.0108>.

- [52] Liam Boyle, Nicolas Baumann, Seonyeong Heo, and Michele Magno. Enhancing lightweight neural networks for small object detection in iot applications. In *2023 IEEE SENSORS*, pages 01–04, 2023. doi: 10.1109/SENSORS56945.2023.10325126.
- [53] Hongrong Cheng, Miao Zhang, and Javen Qinfeng Shi. A survey on deep neural network pruning-taxonomy, comparison, analysis, and recommendations, 2024. URL <https://arxiv.org/abs/2308.06767>.
- [54] PD Meek and A Pittet. User-based design specifications for the ultimate camera trap for wildlife research. *Wildlife Research*, 39(8):649–660, 2012.
- [55] Alexandra Swanson, Margaret Kosmala, Chris Lintott, Robert Simpson, Arfon Smith, and Craig Packer. Snapshot serengeti, high-frequency annotated camera trap images of 40 mammalian species in an african savanna. *Scientific Data*, 2(1):150026, Jun 2015. ISSN 2052-4463. doi: 10.1038/sdata.2015.26. URL <https://doi.org/10.1038/sdata.2015.26>.